J. Fluid Mech. (1996), *vol.* 308, *pp.* 313–340

Manifestations of bottom topography on the ocean surface: the physical mechanism for large scales

By VICTOR I. SHRIRA AND SERGEI Yu. ANNENKOV

P. P. Shirshov Institute of Oceanology, Russian Academy of Sciences, Krasikova 23, Moscow 117218, Russia

(Received 2 August 1994 and in revised form 22 September 1995)

The paper is a first attempt at theoretical investigation of the experimentally observed enigmatic phenomenon of surface manifestations of bottom topography reproducing well the image of the relief despite several kilometres of ocean depth. Both satellite observations and direct measurements have been repeatedly reported in the last two decades. We suggest a possible mechanism for these manifestations in a large scale range (of the order 5×10^1–10^3 km), based on the hydrodynamic theory of quasi-geostrophic stratified flow over topography on a β-plane.

The classical theories of quasi-geostrophic flow over topography on a β-plane do not include vertical shear, and it is well-known that the disturbance caused by topography cannot reach the surface of a stratified ocean unless the stratification or current velocity is unrealistic. The new element changing the situation qualitatively is the taking into account of the influence of near-bottom and near-surface boundary layers, where flow velocities, velocity gradients and stratification can significantly exceed the corresponding values for the flow in the main body. The asymptotic solution derived shows the considerable increase of the normal mode amplitude towards the boundaries. Thus, this specific distortion of the eigenmode structure results in effective forcing of the modes by topography and, on the other hand, leads to pronounced disturbances in the fields of near-surface characteristics. The mechanism effectiveness is demonstrated by the fact that the surface disturbance amplitude normally significantly exceeds the corresponding value for the barotropic current equal to the maximum of the shear flow. A remarkable feature of the solution is that the Green's function is strongly localized in the horizontal plane for a wide range of relevant parameters, thus leading to the close resemblance of surface patterns and bottom relief. To get a better understanding of the quantitative characteristics of the mechanism, the dependence of the effect on the parameters of an N-layer model was studied in detail. The amplification of the surface manifestations due to the presence of boundary layers can reach several orders of magnitude and thus make the manifestations easily observable. The surface temperature anomalies due to topography were estimated and found to be observable under favourable conditions.

1. Introduction

Modern physical oceanography does not provide grounds to assert that a direct link between surface and near-bottom fields may exist, and it is generally assumed that

any resemblance between patterns observed at the surface and bottom topography features is illusive.

However, certain spectacular experimental observations of recent years motivated us to reconsider this common viewpoint. First, from the beginning of intensive manned orbital flights, people who had the benefit of observing the Earth from space repeatedly reported 'underwater mountains' that they were able to discern beneath the ocean surface at a depth of several kilometres. These observations, 'unusual from any traditional point of view' (Solomakha & Fedorov 1983) were initially discarded as impossible: besides the fact that they were never made by specialists in oceanography, no documentary evidence was presented, and information on the conditions of observation was always lacking. Nevertheless, such strange reports, repeated independently by different people with persistence and certainty, could not remain in the field of 'scientific folklore' and eventually gave rise to first attempts at investigation.

These observations have never been systematized, the already cited paper by Solomakha & Fedorov (1983) being probably the only attempt at a serious analysis. These authors stated that the bottom topography cannot be directly visible from space, despite the claims otherwise. Indeed, it is well-known that an underwater object can very rarely be seen beneath the depth of, say, 50 m (e.g. Jerlov 1968); but the actual thickness of the water layer above the mountains so 'observed' sometimes exceeded several kilometres! On the other hand, the possibility that changes in the geoid height due to bottom topography can be observed visually was also disproved by Solomakha & Fedorov (1983); the corresponding tilts of the surface were found to be at least an order of magnitude smaller than those that could be observed. Three more realistic hypotheses were discussed on a qualitative level, the topographically caused disturbances in the surface and subsurface flow fields being their common basis. The authors claimed that the plankton or mud redistribution due to these disturbances may be observable, as well as surface wave modulations, and specified the optimal visibility conditions, but did not point out any mechanism responsible for the formation of such disturbances in the upper layers.

Meanwhile, observations of another kind appeared several years ago, yet did not get attention they merited. It was discovered that there are bands in the one-dimensional spatial spectrum where surface temperature has surprisingly high correlations with the bottom topography (again at several kilometres depth!). This remarkable phenomenon was probably first mentioned in the short note by Paramonov & Lebedeva (1981), who measured surface temperature across the Mid-Atlantic Ridge. Several years later Ilyin & Melnikov (1988) investigated these correlations more thoroughly and found two spectral bands of high correlations: 4–40 km and $>$ 200 km. They also supposed that certain non-specified global mechanisms connecting bottom processes with those in the near-surface layer must exist, and suggested that the appearance of the correlations at shorter scales might be due to the fact that the process of baroclinic tide formation is dominated by topography. Figure 1 shows some typical examples of the existing evidence of the remarkable bottom topography–near-surface temperature correlations. Figure 1 (*a*) was taken from the recent data (Melnikov 1988). However, similar examples can be, in principle, extracted from the vast amount of existing hydrographic data, never analysed from this point of view to our knowledge. Figure 1 (*b*) is based on the data given in the classical atlas (Fuglister 1960). In this paper we concentrate on processes with wavelengths of 10^2–10^3 km, though the ideas can also be applied to somewhat shorter scales.

Thus, an explanation of the observations described above requires first of all

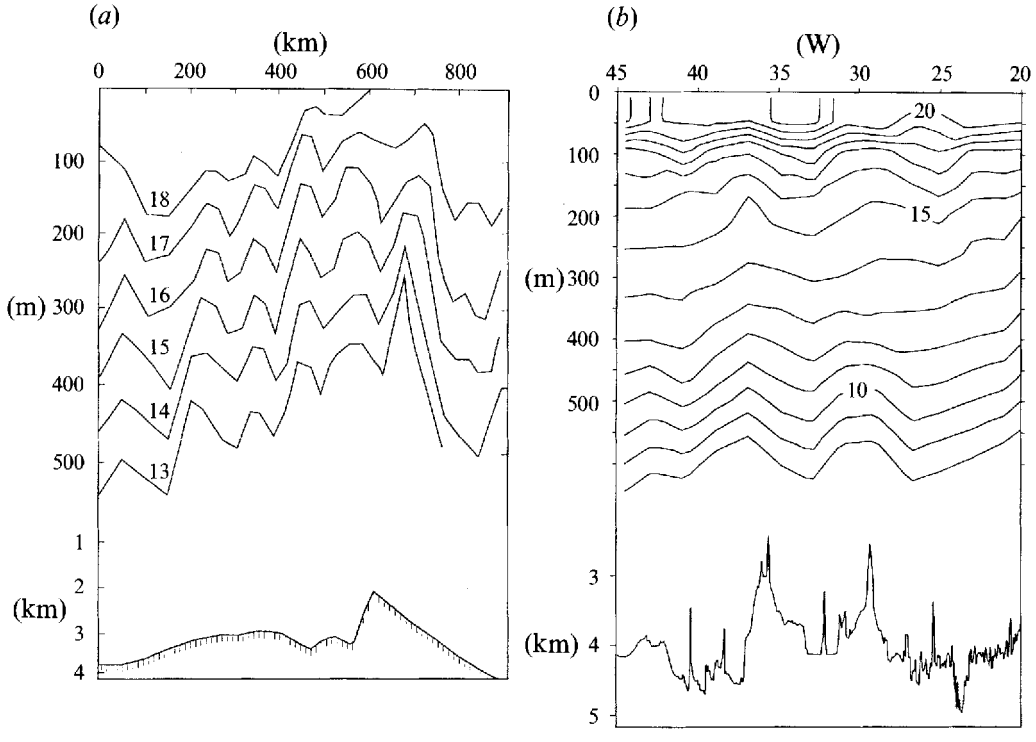

FIGURE 1. Examples of bottom topography manifestations in the near-surface temperature field. (*a*) Temperature profile on a cross-section over the Mid-Atlantic Ridge at 34° N (Melnikov 1988). (*b*) Temperature profile along 32° S, plotted using the data from Fuglister (1960, cf. plot on p. 19.).

a hydrodynamic theory providing a distinct pattern of surface or near-surface flow characteristics closely related to the shape of bottom relief features. This '*hydrodynamic image*' then could be transformed into directly observable features on the surface through a number of mechanisms, some of which are well-known from the study of internal wave manifestations (see e.g. Pelinovsky 1982). In this work we will be concerned with the hydrodynamic part of the problem. In order to explain the observed phenomena, the hydrodynamic theory must:

(i) provide an effective mechanism for the penetration of near-bottom perturbations to the upper layer, and

(ii) this mechanism should give *local* or near-local relations between topography and the flow perturbation at the surface.

These conditions ensure that the topographic image be visible (easily observable), and preserve similarity to the real topography shape.

Our attention will be focused on the *steady patterns*, since they seem more likely to be observed, and it is natural to postulate *a priori* that the mechanism can be found within the stationary model. The scales involved suggest making use of the quasi-geostrophic β-plane approximation; smaller scales will be considered elsewhere.

The theory of rotating stratified flow over topography is a well-established part of classical hydrodynamics. However, most attention in the past was attracted to the case of uniform (f-plane) rotation. Fewer papers were concerned with β-plane flow, probably Ingersoll (1969), McCartney (1975, 1976), Janowitz (1975) and Johnson (1977) being the most important; see Hogg (1980) and Zyryanov (1985) for reviews. The theory is still far from being complete: for instance, no understanding of

the process of time-dependent adjustment of β-plane flow that encounters topography exists, and no numerical work comparable to the famous f-plane investigation of Huppert & Bryan (1976) has been done, to our knowledge.

Nevertheless, the relatively simple problem of steady horizontally uniform zonal quasi-geostrophic flow over low-rise one-dimensional or axisymmetric topography is rather well-studied. This problem is linear, and it is natural to present the solution in the form of a convolution of the corresponding Green's function G and any topography, which is assumed localized. The separation of variables leads to an expression for the horizontal part of G via Bessel functions, in the case of eastward flow supplemented by infinite Fourier–Bessel series representing the wake of stationary Rossby waves behind an obstacle. This distinguishes the β-plane solution from the f-plane one, where there is no wake, at least in the case of horizontally uniform current, and the Green's function is logarithmic, the disturbance being more 'spread' over the horizontal plane.

In the simplest model of vertically uniform current and stratification the exact expression for G is well-known; but attempts to take into consideration the vertical structure of the flow meet the inevitable impediment – the vorticity equation cannot be solved analytically when velocity U and/or Brunt–Väisälä frequency N change with depth. We were unable to find in the literature any successful analysis of shear effects relevant to this problem. The only partial success we are aware of was achieved by Rooney & Janowitz (1979) who managed to take into account the atmospheric wind shear via the modification of boundary conditions. However, a true consideration of vertical shear effects still remains an open problem and, generally speaking, even the direct numerical solution of the stationary problem may be impossible for an arbitrary profile of U, since the details of the evolution towards the stationary state prove to be important.

Thus, we are left with the unsheared incoming zonal current over infinitesimal topography. The explicit solution for this case shows that a disturbance over axisymmetric topography has the shape of a 'Taylor–Hogg cone' (the term proposed by Zyryanov), its amplitude decaying exponentially with the distance from the bottom. The real ocean is rather strongly stratified in this sense, and the cone *usually cannot reach the surface* unless the barotropic current has the speed of 5–10 cm s^{-1}, which is too high for the time- and vertically averaged currents in the ocean.

The new element in the present work changing the situation qualitatively is the taking into account of the specific vertical structure of the flow, viz. the presence of surface and bottom boundary layers. Indeed, the surface layer usually has a current velocity much higher than that of inner layers and is characterized by large gradients of current and stratification; the same, though to a lesser extent, is true for the bottom layer. There is no need to seek corroboration of the former statement, the latter being also supported by observations (see e.g. Dickson *et al.* 1985; Warren & Owens 1985; Klein 1987) and some theoretical models (Barenblatt, Galerkina & Lebedev 1992). However, it is important to note that the lower boundary layer is usually rather weak (at most 3–4 cm s^{-1} on average, though much larger values were observed occasionally, see e.g. Klein 1987). We demonstrate that if the realistic vertical flow shear is taken into account, then the 'transmission' of the disturbance from bottom to surface is found to be considerably higher than for the barotropic flow with the same flux (we term their ratio an '*enhancement coefficient*'), and the characteristics of the upper layer can be significantly distorted by topography. The mechanism turns out to be remarkably effective provided that the boundary-layer structure of the ambient current is sufficiently pronounced, and the enhancement coefficient can exceed 10^1

for geophysically relevant parameter values (examples are shown in figure 5 below). As discussed in § 3.3, the response normally even exceeds that of the barotropic flow equal to the *maximum* of the sheared current. The coefficient attains even larger values for the disturbance velocity at the surface. It is important that the unrealistic bottom current velocity is not needed for the mechanism to work. In order to be assured that experimentally observed flow structures are compatible with the conditions involved in the theoretical predictions, we have carried out an analysis of the dependence of surface disturbance amplitude on the parameters of a three-layer model, which is the simplest one implementing the vertical structure described above. We show that even in the case of relatively low topography the free surface deflection turns out to be of the order of 10^1 cm per 100 km, the variations of the surface current are comparable with the undisturbed values, and the pycnocline displacements can be up to dozens of metres and may be observed visually under certain conditions.

On the other hand, we show that for large enough length scales the ratio between different Fourier harmonics of the topography and their counterparts in the surface perturbation tends to a constant (i.e. the '*transmission coefficients*' for different Fourier harmonics cease to depend upon scale). Thus, the topography is shown on the surface with virtually undistorted large-scale features, producing an impression of 'direct visibility' of large-scale underwater features through the thick water layer.

The paper is organized as follows. Section 2 contains the statement of the problem as a quasi-geostrophic vorticity equation forced at the lower boundary. In § 3 we study the problem within the most general continuous model. For the steady motions that are of prime concern for us nonlinearity in the vorticity equation vanishes identically and the problem reduces to a linear boundary problem, which is treated via the standard normal mode analysis employing, however, the smallness of boundary-layer thicknesses. It is found that the presence of bottom and surface layers with sharp vertical gradients of current and stratification does not change, to the first order of the asymptotic procedure, the dispersion properties of vertical normal modes. Instead, it changes drastically the mode profile within the layers, which becomes proportional to $(U - c)$ there, U and c being the basic current and the phase velocity of the mode. Thus, for the type of vertical structure being considered, the stationary modes acquire 'tails' attached to the horizontal boundaries. These tails result in significant enhancement of the surface manifestations: the bottom tails increase the forcing of the modes by topography while the surface tails lead to more pronounced disturbances of these forced modes in the fields of near-surface characteristics. On the other hand, since the Green's function is found to be strongly localized in the horizontal plane, the surface disturbance preserves the shape of the topography. This fact provides the hydrodynamic grounds for the close similarity observed between surface patterns and bottom relief.

In § 4, in order to clarify the role of various parameters that characterize the basic flow we consider the multi-layer model. We obtain the general expression for the Green's function for an arbitrary step-like velocity profile. This solution is used for the thorough analysis of the properties of the disturbance due to topography in the parameter space of a three-layer model, which was chosen as the simplest one representing the type of vertical structure described above; the direct computations are analysed.

Section 5 gives a brief discussion of the results and their possible applications.

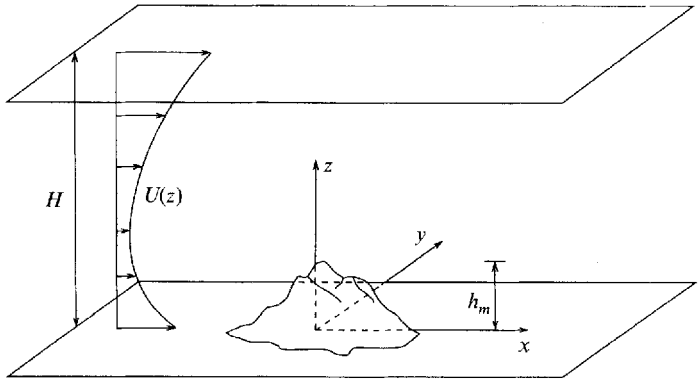

FIGURE 2. Problem statement and basic notation.

2. Basic equations

Let L and U_0 be the length and velocity scales, H the vertical scale, equal to the depth of the fluid, and f_0 and $\beta_0 = \mathrm{d}f_0/\mathrm{d}y$ the Coriolis parameters, where $\beta = \beta_0 L^2/U_0$. The motion depends generally on four non-dimensional parameters: the length-scale ratio $\delta = H/L$, the Rossby numbers $\epsilon = U_0/f_0 L$, $\epsilon_T = 1/Tf_0$, and the Burger number

$$B = \frac{N_0^2\delta^2}{f_0^2} = \frac{gH\Delta\rho}{f_0^2 L^2 \rho_0},$$

where T is a timescale, N_0 is some reference value of the Brunt–Väisälä frequency, $\rho_s(z)$ is a vertical density profile in the undisturbed state, ρ_0 and $\Delta\rho$ are the characteristics of this undisturbed profile, namely the Boussinesq reference density and a measure of vertical changes.

With a Cartesian frame (x, y, z) having its origin on the bottom (with topography removed), where x increases to the east, y to the north, and z upward (see figure 2), motions of inviscid incompressible fluid with a rigid lid on the surface at $z = 1$ are governed by the equations

$$\left.\begin{aligned}
&\epsilon_T \frac{\partial u}{\partial t} + \epsilon \boldsymbol{q}\cdot\nabla u - (1+\epsilon\beta y)v = -\frac{\partial p}{\partial x},\\
&\epsilon_T \frac{\partial v}{\partial t} + \epsilon \boldsymbol{q}\cdot\nabla v + (1+\epsilon\beta y)u = -\frac{\partial p}{\partial y},\\
&\epsilon_T\delta^2 \frac{\partial w}{\partial t} + \epsilon\delta^2 \boldsymbol{q}\cdot\nabla w = -\frac{\partial p}{\partial z} - \rho,\\
&\epsilon \boldsymbol{q}\cdot\nabla\rho + Bw\frac{\mathrm{d}\rho_s}{\mathrm{d}z} = 0,\\
&\nabla\boldsymbol{q} = 0.
\end{aligned}\right\} \tag{2.1}$$

The velocity $\boldsymbol{q} = \{u, v, w\}$, pressure p and density ρ are assumed to be dimensionless, while their dimensional counterparts (denoted by an asterisk) can be obtained as

$$\left.\begin{aligned}
&\{x^*, y^*, z^*\} = L\{x, y, z\}, \qquad \{u^*, v^*, w^*\} = U_0\{u, v, \delta w\},\\
&p^* = \rho_0 U_0 f_0 L p(x, y, z), \qquad \rho^* = [\rho_s(z) + \frac{\epsilon}{B}\rho(x, y, z)]\Delta\rho.
\end{aligned}\right\} \tag{2.2}$$

To simplify the notation, we introduce a function which comprises the stratification

effects

$$S(z) = -B\frac{\mathrm{d}\rho_s}{\mathrm{d}z}.$$

The formulation is completed by the conditions at rigid boundaries

$$\left.\begin{aligned} w &= \boldsymbol{q}\cdot\nabla h, \quad & z &= h(x,y), \\ w &= 0, & z &= 1. \end{aligned}\right\} \tag{2.3}$$

Expansion of the dependent variables in powers of ϵ leads to the vorticity equation

$$\left(\frac{\epsilon_T}{\epsilon}\frac{\partial}{\partial t} + \frac{\partial p}{\partial x}\frac{\partial}{\partial y} - \frac{\partial p}{\partial y}\frac{\partial}{\partial x}\right)\left(\nabla^2 p + \frac{\partial}{\partial z}\frac{1}{S}\frac{\partial p}{\partial z} + \beta y\right) = 0 \tag{2.4}$$

with the boundary conditions

$$\left.\begin{aligned} J\left(p, \frac{\partial p}{\partial z}\right) &= 0, & z &= 1, \\ J\left(p, \frac{\partial p}{\partial z}\right) + SJ\left(p, \frac{h}{\epsilon}\right) &= 0, & z &= h(x,y), \end{aligned}\right\} \tag{2.5}$$

where $J(a,b) = a_x b_y - a_y b_x$.

We are concerned with the quasi-stationary disturbances of large ($\delta = 10^{-1}$–10^{-2}) horizontal scale caused by topography to a steady incoming zonal flow with vertical shear $U(z)$ and assume that the quasi-geostrophic approximation is valid. This means directly that $\epsilon_T \leqslant \epsilon \ll 1$ and also imposes constraints on the disturbance structure, since quasi-geostrophy implies motions of slow speed with gentle sloping of isopycnic surfaces. In order to satisfy these limitations, it will be generally assumed that $B \geqslant O(1)$.

3. General case of continuous stratification

3.1. *Analysis of the vorticity equation*

There are two common ways to deal with the problem (2.4)–(2.5). The first, applied usually for the study of linear Rossby waves over infinitesimal topography, consists in the linearization of (2.4) and (2.5) about the upstream conditions, assuming $\epsilon_T/\epsilon = O(1)$, and searching for the solutions of the type

$$\psi = \mathrm{Re}\{\phi(z)\exp[\mathrm{i}(kx + ly + \omega t)]\},$$

where ψ denotes the perturbation streamfunction, $p(x,y,z) = -U(z)y + \psi(x,y,z)$. This procedure yields the linearized vorticity equation

$$\sigma\left[-k_h^2\phi + \left(\frac{\phi'}{S}\right)'\right] - \left(\frac{\sigma'}{S}\right)'\phi + \beta\phi = 0 \tag{3.1}$$

with the boundary conditions

$$\phi' - \frac{\sigma'\phi}{\sigma} = 0, \qquad z = 1, \tag{3.2a}$$

$$\phi' - \frac{\sigma'\phi}{\sigma} = -\frac{Sh}{\epsilon}, \quad z = 0. \tag{3.2b}$$

Here the prime denotes differentiation with respect to z, $c = \omega/k$, $\sigma = U - c$, and the lower boundary condition has been transferred onto the undisturbed bottom.

On the other hand, it is easy to see that the problem is *naturally linearized* just by omitting its non-steady part. Since we are interested mainly in quasi-stationary disturbances caused by topography, we can put $\epsilon_T \ll \epsilon$ in (2.4), and so obtain

$$J\left(p, \nabla^2 p + \frac{\partial}{\partial z}\frac{1}{S}\frac{\partial p}{\partial z} + \beta y\right) = 0, \tag{3.3}$$

or

$$\nabla^2 p + \frac{\partial}{\partial z}\frac{1}{S}\frac{\partial p}{\partial z} + \beta y = F(p), \tag{3.4}$$

where $F(p)$ is an arbitrary function. Assuming the absence of closed streamlines above topography, we easily obtain

$$F(p) = \frac{p}{U}\frac{\mathrm{d}}{\mathrm{d}z}\frac{1}{S}\frac{\mathrm{d}U}{\mathrm{d}z} - \beta\frac{p}{U}, \tag{3.5}$$

and, again denoting the perturbation streamfunction by ψ, get

$$\nabla^2\psi + \frac{\partial}{\partial z}\frac{1}{S}\frac{\partial\psi}{\partial z} + \frac{\beta - \dfrac{\mathrm{d}}{\mathrm{d}z}\dfrac{1}{S}\dfrac{\mathrm{d}U}{\mathrm{d}z}}{U}\psi = 0 \tag{3.6}$$

with the boundary conditions

$$\frac{\partial\psi}{\partial z} - \frac{\psi}{U}\frac{\mathrm{d}U}{\mathrm{d}z} = 0, \qquad z = 1, \tag{3.7a}$$

$$\frac{\partial\psi}{\partial z} - \frac{\psi}{U}\frac{\mathrm{d}U}{\mathrm{d}z} = -\frac{Sh}{\epsilon}, \quad z = h(x, y), \tag{3.7b}$$

and Long's condition of no upstream influence is also required.

It is obvious that the transition from (3.3) to (3.6) is possible only when all streamlines originate upstream. The question of whether the solution of this stationary problem with closed streamlines found *a posteriori* is applicable has a long history (see e.g. discussions in Hogg 1973, § 7; McCartney 1975; Zyryanov 1985). It appears to be well-established now that if a closed streamline emerges in the flow, the viscous effects will eventually kill off the motion within it, and a stagnant region will be formed, separated from the rest of the flow by the so-called Stewartson boundary layers. The inviscid solution is thus indeterminate in principle; however, it seems reasonable to assume that the inviscid flow within the closed streamlines 'memorizes' the state 'just before' the streamline was closed and this part of the flow was isolated. Then equation (3.6) may be applicable (in any case, it is applicable on any streamline that originates upstream). Following the usual practice, this difficulty is ignored below.

The boundary-value problem (3.6)–(3.7 *a*, *b*) is hardly tractable analytically in the general case; however, certain additional assumptions that can give essential gains in simplicity are consistent with our purposes. First, we assume that the homogeneous counterpart of the problem does not possess baroclinic instability, i.e. the imaginary part of the phase velocity is equal to zero; this does not lead to loss of definiteness since the corresponding sufficient conditions for a quasi-geostrophic model can be stated explicitly (this is not the case for a general nearly geostrophic model). For our purposes, it is enough just to bear in mind that the point $c = 0$ should lie outside (and somewhat distant from) the 'semicircle' for the phase speed of an unstable mode. Certainly, this estimate could be more precise (see Gnevyshev & Shrira 1990).

Consequently, we require that the current be unidirectional, so that its velocity cannot vanish anywhere in the flow.

Second, we shall 'transfer' for simplicity the lower boundary condition onto the undisturbed bottom, following numerous earlier studies (Johnson 1977; Zyryanov 1985), although the exact boundary condition could easily be taken into account. The thorough comparison of two solutions carried out in a different context by Schar & Davies (1988) led to the conclusion that within the quasi-geostrophic approximation the two flow fields are 'commensurate', i.e. the 'simplified' boundary condition merely distorts the mountain shape without significant changes in the solution structure. Actually, the quasi-geostrophy itself limits the solution in a way that makes the use of exact lower boundary condition excessive – the solution for infinitesimal topography is valid for higher obstacles provided that the flow does not leave the quasi-geostrophic regime. Thus, the boundary condition (3.7*b*) will be applied on the surface $z = 0$.

Applying to (3.6)–(3.7*a*, *b*) the Fourier transform in (x, y), we find for the transformed streamfunction $\tilde{\psi}(k, l, z)$

$$\frac{\partial}{\partial z}\left(\frac{1}{S}\frac{\partial \tilde{\psi}}{\partial z}\right) + \left(-k^2 + \frac{\beta - \dfrac{\mathrm{d}}{\mathrm{d}z}\dfrac{1}{S}\dfrac{\mathrm{d}U}{\mathrm{d}z}}{U}\right)\tilde{\psi} = 0 \tag{3.8}$$

and

$$\left.\begin{aligned} &\frac{\partial \tilde{\psi}}{\partial z} - \frac{\tilde{\psi}}{U}\frac{\mathrm{d}U}{\mathrm{d}z} = 0, \qquad z = 1, \\ &\frac{\partial \tilde{\psi}}{\partial z} - \frac{\tilde{\psi}}{U}\frac{\mathrm{d}U}{\mathrm{d}z} = -\frac{S\tilde{h}}{\epsilon}, \qquad z = 0. \end{aligned}\right\} \tag{3.9}$$

The solution of the problem (3.6)–(3.7*a*, *b*) then can be written as

$$\psi(x, y, z) = \int_{-\infty}^{+\infty}\int_{-\infty}^{+\infty} G(x - \xi, y - \eta, z)h(\xi, \eta)\,\mathrm{d}\xi\mathrm{d}\eta, \tag{3.10}$$

where the Green's function $G(x, y, z)$ is obtained via the solution of (3.8), (3.9) when $\tilde{h} \equiv 1$ is formally set. This can be solved numerically for arbitrary $S(z)$, $U(z)$ (recall that we exclude the cases with $U = 0$ at some z); the solution for $S = \text{const}$, $U = \text{const}$ can be found in Johnson (1977), Zyryanov (1985). Thus, the solution of the nonlinear forced quasi-geostrophic problem (3.3) consists of the stationary Rossby waves represented by ($c \equiv 0$) solutions of the linearized problem (3.1)–(3.2), but with the homogeneous boundary conditions instead of (3.2*b*). The fact that the nonlinear terms are found to be identically equal to zero is due to the neglect of time-dependence and to the uniformity of the incoming flow; the situation here closely resembles that of two-dimensional stationary Boussinesq flow over topography, when the nonlinear terms also vanish provided that the stratification is uniform (Grimshaw & Yi 1991).

Consequently, in order to obtain the Green's function for (3.6)–(3.7*a*, *b*), it is necessary first to study the properties of the linearized problem (3.1)–(3.2) for $c = 0$ and $h \equiv 0$. Since the phase velocity is fixed, the squared wavenumber k_h^2 acts as an eigenvalue, the special feature of the problem being in the fact that real and imaginary values of k_h are equally important. Indeed, they both correspond to poles in the integrand of (3.10), real k giving those on the real axis, thus yielding a wake of trapped Rossby waves behind the obstacle. In the next subsection we, however,

release the limitation $c = 0$, since the analysis there is carried out for the general case of (3.1).

3.2. *Asymptotic analysis: boundary-layer-type asymptotics*

In this subsection our attention will be focused on the normal mode solution of the homogeneous boundary-value problem for the vorticity equation (3.1). We consider the case when the functions $U(z)$, $S(z)$ vary slowly over the entire fluid depth except for the narrow layers (of dimensionless depths Δ_1, Δ_2) near the boundaries $z = 0, 1$ respectively, where the gradients of these functions are localized.

It is convenient to write

$$\left.\begin{aligned} U(z) &= U^*\left(\frac{1-z}{\delta_2}\right) U_*\left(\frac{z}{\delta_1}\right) U_i(\mu z), \\ S(z) &= S^*\left(\frac{1-z}{\delta_2}\right) S_*\left(\frac{z}{\delta_1}\right) S_i(\mu z), \end{aligned}\right\} \tag{3.11}$$

where $\delta_1 = k_h\Delta_1$, $\delta_2 = k_h\Delta_2$, μ measures the 'outer' depth scale, i.e. the characteristic scale of depth over which the interior functions change, $\mu \ll \min(\delta_1, \delta_2)$, indices '$_*$' and '*' correspond to lower and upper boundary layers, respectively, and we assume, without loss of generality, that $U(z) = U_i$, $S(z) = S_i$ outside the boundary layers (i.e. the 'fast' functions in the right-hand side tend to 1 as their arguments approach infinity). Here and below the term 'interior' is used for the functions that characterize the main body of the flow.

Consider now the vicinity of, say, the lower boundary. The problem is posed by the equation

$$\sigma\left[-k_h^2\phi + \left(\frac{\phi'}{S}\right)'\right] - \left(\frac{\sigma'}{S}\right)'\phi + \beta\phi = 0, \tag{3.12}$$

where $\sigma \equiv U - c$, with the boundary conditions

$$\sigma\phi' - \sigma'\phi = 0, \qquad z = 0, 1, \tag{3.13}$$

where $U(z)$ and $S(z)$ are assumed to vary only within the layer of depth Δ near the bottom $z = 0$, so that $\Delta \ll 1$ and $k\Delta \ll 1$. Using the asymptotic technique of Shrira (1989), we expand ϕ, σ and the operator $\mathrm{d}/\mathrm{d}z$ in the form

$$\left.\begin{aligned} \phi &= \sum_{i=0}^{\infty} \delta^i \phi^{(i)}, \qquad \sigma = \sigma_0 - \delta c_1 - \delta^2 c_2 - \ldots, \\ \frac{\mathrm{d}}{\mathrm{d}z} &= \frac{1}{\delta}\frac{\partial}{\partial z_0} + \frac{\partial}{\partial z_1}, \end{aligned}\right\} \tag{3.14}$$

where $\delta = k\Delta$, z_0 and z_1 correspond to 'inner' (i.e. within the sheared layer) and 'outer' depth scales, respectively. At the zeroth order the equation yields

$$\sigma_0 \frac{\partial}{\partial z_0}\left(\frac{1}{S}\frac{\partial \phi^{(0)}}{\partial z_0}\right) - \phi^{(0)}\frac{\partial}{\partial z_0}\left(\frac{1}{S}\frac{\partial \sigma_0}{\partial z_0}\right) = 0. \tag{3.15}$$

The fundamental system of solutions for this equation is

$$\phi^{(0)} = A_0\sigma\int_0^{z_0} \frac{S\,\mathrm{d}z'}{\sigma_0^2} + B_0\sigma_0, \tag{3.16}$$

where A_0 and B_0 are arbitrary functions of z_1; (3.13) gives $A_0 \equiv 0$. So at this order

the 'inner' solution takes the form

$$\phi^{(0)} = \sigma_0 f(z_1) \tag{3.17}$$

where the eigenvalue c_0 and the function f are as yet arbitrary.

At the next order we formally obtain

$$\phi^{(1)} = -\frac{\partial f}{\partial z_1}\sigma_0 z_0 - c_1 f. \tag{3.18}$$

Since we have assumed that $U - c_0 \neq 0$, it follows that $\partial f/\partial z_1 \equiv 0$; but c_0 and f are still arbitrary, and so the last term on the right-hand side of (3.18) can be absorbed into (3.17), the first-order approximations to ϕ and c being identically zero. Thus, $\phi^{(1)} = 0$, and we have also obtained the lower boundary condition for the outer solution. In order to get the eigenvalue c_0, we have to move up to the second order. After some algebra, one finds that

$$\phi^{(2)} = \sigma_0 f \int^{z_0} \frac{S\int_0^{z''} (\sigma_0^2 k_h^2 - \sigma_0 \beta)\,\mathrm{d}z'}{\sigma_0^2}\mathrm{d}z'' - \sigma_0 \frac{\partial^2 f}{\partial^2 z_1}\int^{z_0} \frac{S\int_0^{z''} \frac{\sigma_0^2\,\mathrm{d}z'}{S}}{\sigma_0^2}\mathrm{d}z'' - f c_2 + B_2\sigma_0, \tag{3.19}$$

with B_2 arbitrary. The right-hand side must remain finite as $z_0 \to \infty$; this requirement leads to the dispersion relation

$$\frac{\partial^2 f}{\partial^2 z_1} + S\left(-k_h^2 + \frac{\beta}{\sigma_0}\right) f = 0. \tag{3.20}$$

Together with the boundary conditions

$$\frac{\partial f}{\partial z_1} = 0, \qquad z_1 = 0, 1 \tag{3.21}$$

this determines f and c_0 and completes the solution. The other boundary layer is treated analogously. Let us then summarize the results:

(i) The leading-order solution has the form

$$\phi(z) = \phi^*\left(\frac{1-z}{\delta_2}\right)\phi_*\left(\frac{z}{\delta_1}\right)\phi_i(z), \tag{3.22}$$

where

$$\phi^*\left(\frac{1-z}{\delta_2}\right) = \frac{U^*\left(\frac{1-z}{\delta_2}\right) - c}{1-c}, \quad \phi_*\left(\frac{z}{\delta_1}\right) = \frac{U_*\left(\frac{z}{\delta_1}\right) - c}{1-c}, \tag{3.23}$$

so that $\phi(z) \to \phi_i(z)$ as $\delta_1 \to 0$, $\delta_2 \to 0$. This form describes the distortion of the normal mode within the boundary layers; note that this result is independent of the $S(z)$ profile.

(ii) $\phi_i(z)$ is given by the standard boundary value problem (3.20)–(3.21) without the boundary layers, being merely the familiar trigonometric solution for the case when U and S are constant.

(iii) The dispersion properties of the solution are completely determined by its interior part (using this term in the aforementioned sense), and are unaffected by the boundary layers, to the second order in δ_1, δ_2.

We note that the problem considered differs from the analogous boundary-layer problem for the Rayleigh equation in the classical theory of hydrodynamic stability,

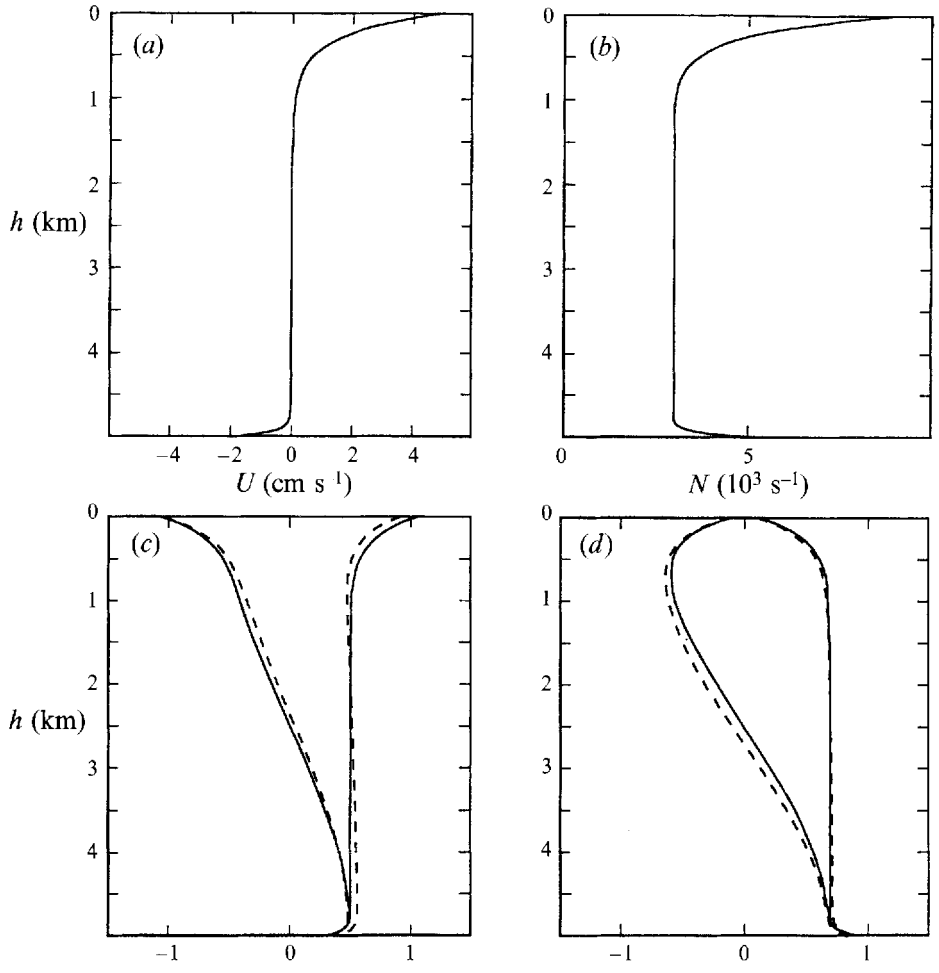

FIGURE 3. Mode distortion for the 'antisymmetric' basic currents: asymptotic (solid lines) and numerical (dashed lines) solutions of the boundary value problem (3.12), (3.13). (*a*) The specific current profile $U(z)$ with the 'antisymmetric' boundary-layer structure, used in this example. (*b*) The Brunt–Väisälä frequency profile $N(z)$. (*c*) Barotropic and first baroclinic modes for $c = -4.33$ cm s^{-1}, corresponding to the (numerical) eigenvalues $k_h^2 = 3.48 \times 10^{-10}$ m^{-2} and $k_h^2 = -4.43 \times 10^{-11}$ m^{-2}. (*d*) The same for negative $(U - c)$ values, $c = 5.98$ cm s^{-1}, $k_h^2 = -2.75 \times 10^{-10}$ m^{-2} and $k_h^2 = -8.07 \times 10^{-10}$ m^{-2}.

owing to the specific form of boundary conditions (3.2) (but, incidentally, the problem for the Rayleigh equation *with a free surface* is similar to the problem considered, see Appendix to Shrira 1993). Indeed, no solution of the 'vorticity wave' type appears. Moreover, the only consequence of a boundary layer imposed on the slowly varying current and density profiles is that the vertical mode gets attached to the inner sides of the boundary layers as if they were solid (satisfying the boundary condition $\mathrm{d}\phi_i/\mathrm{d}z = 0$, the solution within the layers being proportional to $(U-c)$, to the leading order, thus forming 'tails' affixed to either end of a slowly varying function.

To illustrate the result, the solution of the boundary-value problem for the particular functions $U(z)$, $N(z)$ (figure 3 *a, b*) is presented in figure 3 (*c, d*) for two different values of c (solid curves); the barotropic and first baroclinic modes are shown. In fact, the only 'wave-like' mode (i.e. with $\kappa_h^2 > 0$) is the barotropic mode in case (*c*), and

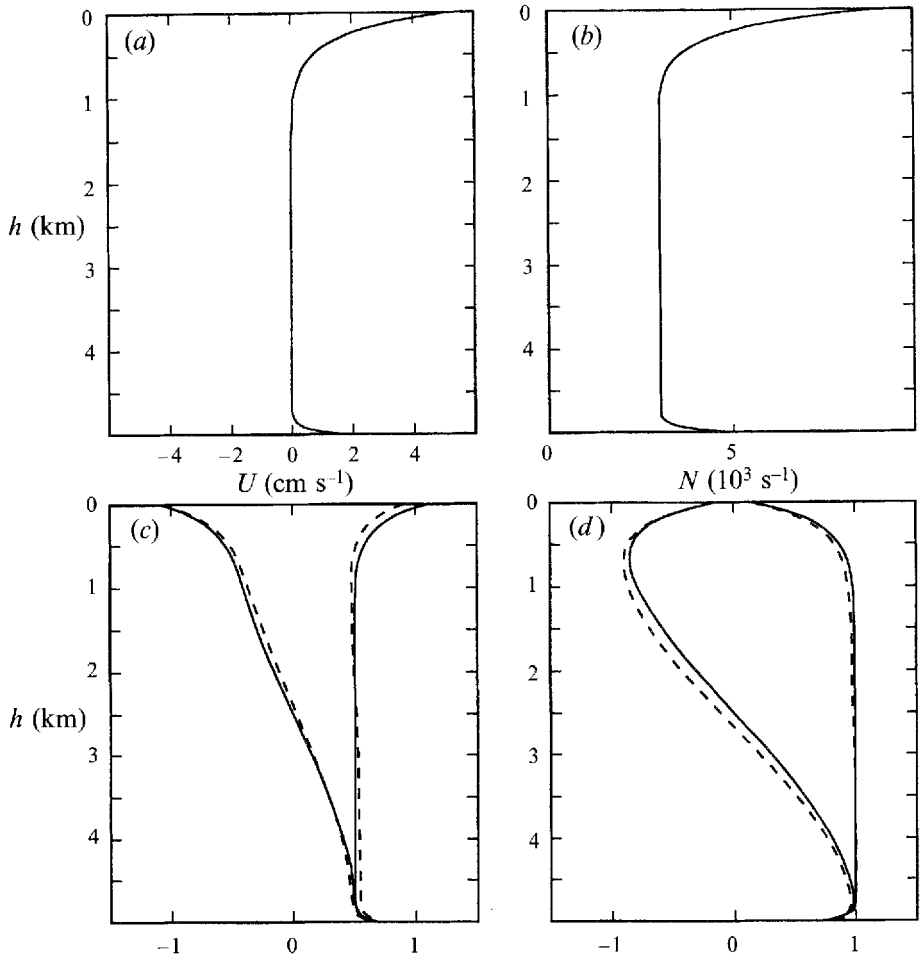

FIGURE 4. Mode distortion for the 'symmetric' basic currents: asymptotic (solid lines) and numerical (dashed lines) solutions of the boundary value problem (3.12), (3.13) for another basic type of vertical structure $U(z)$, $N(z)$. (*a*) Current profile $U(z)$ with the 'symmetric' boundary-layer structure, used in this example. (*b*) The Brunt–Väisälä frequency profile $N(z)$. (*c*) Barotropic and first baroclinic modes for $c = -4.33$ cm s^{-1}, corresponding to the (numerical) eigenvalues $k_h^2 = 3.46 \times 10^{-10}$ m^{-2} and $k_h^2 = -3.85 \times 10^{-11}$ m^{-2}. (*d*) The same for negative $(U - c)$ values, $c = 5.98$ cm s^{-1}, $k_h^2 = -2.77 \times 10^{-10}$ m^{-2} and $k_h^2 = -8.23 \times 10^{-10}$ m^{-2}.

in case (*d*) only the spatially decaying modes are possible; it is worthwhile noting that wave-like and decaying modes are equally important for the forced problem. For comparison, the direct numerical solutions, obtained with a staggered-mesh finite-difference scheme, are given (dashed curves). Another example is shown in figure 4 (*a–d*), where the boundary layers have different shear signs. It is seen that, in general, the modes have local extrema near the boundaries, their signs coinciding with those of the function $(U - c)$.

3.3. *The forced problem*

In this subsection the result obtained is applied to the problem (3.6)–(3.7 *a, b*). Provided that the functions $U(z)$, $S(z)$ can be presented in the form considered in the preceding subsection, the Green's function can be calculated directly. It is obvious that, in order to be effectively forced by topography, a natural mode of the system must have

non-zero amplitude in the vicinity of the bottom, and the degree of forcing depends directly on this amplitude. On the other hand, the modes that have a maximum at or near the surface are most easily observed, providing the basis for the bottom topography manifestations in the surface field.

Thus, taking into account narrow shear layers near the horizontal boundaries helped us to point out the class of situations when the response to the topography in the surface and subsurface fields is significantly enhanced. Certainly, this rather qualitative conclusion is unable to explain on its own the high surface fields–topography correlations mentioned earlier, investigations of the dependence of the Green's function on horizontal coordinates being necessary.

If the complete orthonormalized set of normal modes $\phi_i(z)$ with the corresponding eigenvalues κ_i is known, then, expanding the solution over the eigenmodes of the homogeneous problem, we obtain the Green's function in the form

$$G(x,y,z) = -\frac{1}{4\pi^2\epsilon}\int\left[\sum_{i=0}^{\infty}\frac{\phi_i(0)}{k_1^2+k_2^2-\kappa_i^2}\phi_i(z)\right]\exp(ik_1x+ik_2y)\,dk_1dk_2, \tag{3.24}$$

and the integration in (3.24) gives

$$G(R,\theta,z) = \hat{G}(R,z) + F(R,\theta,z), \tag{3.25}$$

where

$$\hat{G}(R,z) = \frac{1}{2\pi\epsilon}\left(-\frac{\pi}{2}\sum_{i=0}^{N}Y_0(\kappa_iR)\phi_i(0)\phi_i(z) + \sum_{i=N+1}^{\infty}K_0(\kappa_iR)\phi_i(0)\phi_i(z)\right) \tag{3.26}$$

and

$$F(R,\theta,z) = -\frac{1}{\pi\epsilon}\sum_{i=0}^{N}\left[\sum_{m=0}^{\infty}\frac{\cos[(2m+1)\theta]J_{2m+1}(\kappa_iR)}{2m+1}\right]\phi_i(0)\phi_i(z), \tag{3.27}$$

where $(x,y) = R(\cos\theta, \sin\theta)$, N is the number of the highest wave-like mode, Y_0 and K_0 are the Neumann and MacDonald functions, respectively, J_m is the Bessel function of the first kind, and $F(R,\theta,z)$ is the part of the Green's function corresponding to the wake behind the obstacle.

The form of the Green's function, as obtained in (3.25)–(3.27), together with the results of § 3.2 allow to formulate the effect of the boundary layers on the stationary disturbance forced by topography. As the behaviour of each mode in the boundary layers does not depend on the wavevector and the mode number, one can easily establish a direct connection between the solutions of the forced problem with and without boundary layers for arbitrary topography similar to that between the solutions of the homogeneous problem (3.22), (3.23),

$$\psi = \psi_i(z)\frac{U(0)}{U_0}U_*\left(\frac{z}{\delta_1}\right)U^*\left(\frac{1-z}{\delta_2}\right),$$

where ψ is the solution of the inhomogeneous problem with the boundary layers, ψ_i is the solution for the same topography with the boundary layers neglected, U_* and U^* have the same sense as above, and U_0 is the interior current value.

Thus, the interior solution is multiplied by $U(0)$. However, the disturbance within the boundary layers is much larger, since it is again multiplied by $U(z)$, and hence the simultaneous presence of surface and bottom boundary layers must lead to pronounced surface patterns.

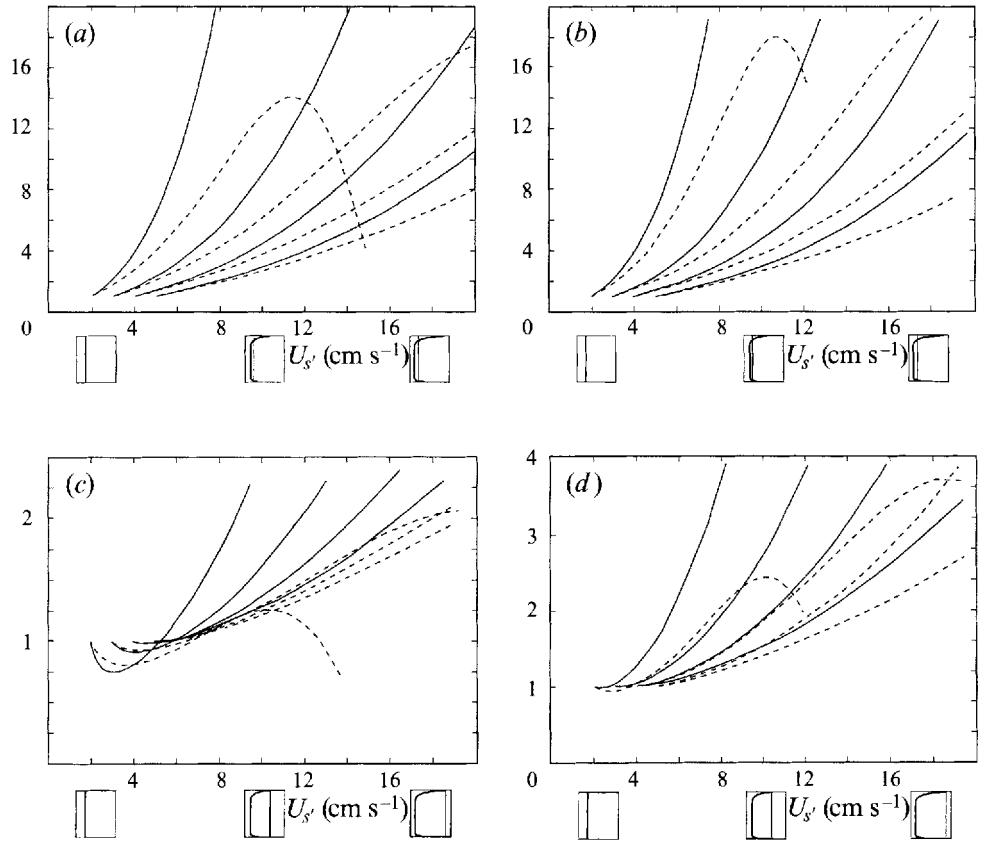

FIGURE 5. Normalized disturbance maximum (a and c) and its horizontal gradient maximum (b and d) *vs.* basic current surface velocity for the westward flow over an axisymmetric isolated obstacle. The leftmost point of each curve corresponds to the barotropic flow, the velocity integral over depth being kept constant along the curves. The values are normalized by the corresponding values for the barotropic flow with the same flux (a, b) and for the barotropic flow equal to the maximum of the sheared current (c, d). Asymptotic curves are solid; numerical curves are dashed. The sketches illustrate the change of vertical structure and the barotropic flow used for normalization.

In order to estimate the response enhancement due to the mechanism described, the amplitude of the disturbance caused by an axisymmetric isolated topography to the westward flow with boundary layers was compared with that for the 'equivalent' barotropic flow, the latter being defined as the barotropic flow with the same flux as the baroclinic one under consideration. The upper-boundary-layer thickness was taken to be about 150 m, while the thickness and velocity of the lower boundary layer were equal to $\frac{1}{2}$ and $\frac{1}{3}$ of the corresponding surface values. The maximal amplitudes of the pressure disturbance and velocity were computed, both asymptotically and numerically; the ratios to the corresponding values in the equivalent barotropic current (*enhancement coefficients*) are shown in figure 5(a, b) respectively for four values of westward flow average. The degree of the 'boundary-layer nature' of the flow is measured via the surface velocity U_s. The geophysically relevant enhancement is of one order in magnitude, though the averaged current should not approach zero, since then the link between two boundary layers becomes weak and the mechanism ceases to work. It is noteworthy that the enhancement for the velocity field is

roughly two times more pronounced than that for the pressure disturbance or surface elevation.

The mechanism effectiveness is best demonstrated via the comparison of the disturbances maxima with those for the barotropic current equal to the *maximum* of the shear flow. Results are shown in figure 5(*c*, *d*). Again, the asymptotic solution overestimates the disturbance values to some extent; however, it is remarkable that even the values obtained numerically are normally larger for the shear current than for the 'maximum barotropic' one. As noted above, this enhancement is most apparent for the velocity field.

The cases of westward ($U(z) < 0$) and eastward flow are obviously quite different, the latter being somewhat more complicated. The disturbance in the westward current caused by an axisymmetric obstacle is also axisymmetric, with the maximum over the obstacle centre, and decays like $\exp[-(\min|\kappa_i^2|)^{1/2}R]$. When the current is eastward, at least one of the κ_i^2 is positive, and the wake of stationary Rossby waves exists, significantly distorting the surface disturbance. For a class of eastward flow configurations comprising most of the geophysically relevant situations, the wake consists of the barotropic mode only (that is, $N = 0$), being more rarely supplemented by the first baroclinic one.

Though the wake is an important feature of the solution, its appearance does not seem to be of prime importance to main objectives of this paper. Indeed, the wake consists of stationary eddies of differing signs and is controlled by the barotropic (and perhaps first baroclinic) wavenumber, not by the shape of the topography. The wake behind a real topographic obstacle, usually having a very corrugated form, is unlikely to be observed, since the response would be produced by the sum of vortex chains with close length scales and virtually random amplitudes and phases. We note that this argument is commonly used for the explanation of the observed absence of wakes behind large seamounts in the ocean (see e.g. Roden 1991).

The response corresponding to the axisymmetric part of the Green's function defined by (3.26) is more crucial for the present study. An important feature of (3.26) is that, since the functions Y_0, K_0 are both strongly localized near the origin, the Green's function has the form of a rather sharp impulse. Actually, the function $\hat{G}(R, z)$ may either decay exponentially from the origin or oscillate, but in any case it has a 'delta-like' form, the response (3.10) being close to the shape of the topography, with the shorter scales suppressed.

In order to make this statement more precise, consider the interaction of a single normal mode with topography of unit height comprising one Fourier mode in each horizontal direction

$$h(x, y) = \cos(k_1 x)\cos(k_2 y). \tag{3.28}$$

Calculating the convolution in (3.10), we easily obtain, for the decaying mode ($\kappa_i^2 < 0$), that the response has the form

$$\phi_i(x, y, 1) = \frac{\text{const}}{k_1^2 + k_2^2 - \kappa_i^2}\cos(k_1 x)\cos(k_2 y), \tag{3.29}$$

where the constant depends on the model parameters.

It is seen that each harmonic of the topography is reproduced on the surface with the '*transmission coefficient*' $\mathscr{T}$,

$$\mathscr{T} = \frac{1}{k_1^2 + k_2^2 - \kappa_i^2}.$$

Since $\kappa_i^2 < 0$, the coefficient is limited from above; thus the normal mode serves as a 'low-pass filter' for the topography. The largest topography scales, $O(k_1^2+k_2^2) \ll O(-\kappa_i^2)$, are transmitted almost undistorted, while the shorter scales are suppressed.

The wave-like modes ($\kappa_i^2 > 0$), provided that they are possible in the system, make the situation more complicated. Consider first the radial part of the Green's function $\hat{G}_i(R, z)$ for the ith mode. If $\min(k_1^2, k_2^2) > \kappa_i^2$, the same result (3.29) is easily obtained. In the case of smaller k_1^2 or k_2^2, compactness of topography is necessary for definiteness; it can be shown, however, that the proper cutting of the topography (3.28) at some large distance from the origin again leads to the formula (3.29), provided that the resonant cases $\kappa_i^2 = k_1^2$, $\kappa_i^2 = k_2^2$, and $\kappa_i^2 = k_1^2 + k_2^2$ are excluded. Now the same result (3.29) corresponds to more complex transmission, since the transmission coefficient is not limited and changes sign at $k_1^2 + k_2^2 = \kappa_i^2$. For a one-layer model this means that the large-scale topography is shown on the surface 'inversely', mountains on the bottom corresponding to negative pressure anomalies. Shorter scales are transmitted normally, as in the decaying mode case, but the spectral band near κ_i^2 is enhanced.

It is obvious, however, that the wake produced by the wave-like mode would distort the topographic image being considered. The analysis for the two-dimensional sinusoidal topography is cumbersome; but in the simpler one-dimensional case

$$h(x) = \cos(kx)$$

the result is just

$$\phi_i(x, y, 1) = \frac{\text{const}}{k^2 - \kappa_i^2} \left[\cos(kx) + A\cos(\kappa_i x)\right],$$

where the coefficient A, in general, depends on k, κ_i and the support of h (i.e. the set of all x for which $h(x) \neq 0$). Thus, the wake adds just one extra harmonic to the solution (recall that here we consider the solution for one normal mode over one Fourier harmonic in the bottom relief).

3.4. *Discussion*

The asymptotic analysis of the boundary-value problem (3.6)–(3.7 *a, b*) with the special (and geophysically relevant) structure of the functions $U(z)$, $S(z)$ allowed us to obtain a solution that meets the requirements formulated in the introduction. First, we have found that the boundary-layer structure of the incoming flow provides great enhancement of the surface disturbance that would be otherwise extinguished by stratification. Second, the analysis of the forced problem led to the conclusion that this disturbance represents a virtually perfect 'hydrodynamic image' of the topography, this property being clearly attributed to the fact that the Green's function has a 'delta-like' dependence on the horizontal coordinates. Therefore, we have pointed out an effective mechanism for the surface manifestation of bottom topography. Now we will discuss certain problems and limitations associated with our approach.

An important feature of the solution is that the amplitude of the surface disturbance strongly depends on the existence of narrow (100–300 m) boundary layers, the presence of these layers in the ocean being justified by observations. However, since the normal mode approach is used throughout this paper, we must bear in mind that this approach ceases to be valid when the characteristic time for the formation of a normal mode exceeds the timescale over which these boundary layers exist. A very rough estimate of the characteristic time τ of a mode formation could be found through calculation within the WKB-approximation of the time for a wave packet to cross the ocean from surface to the bottom. Actually, the vertical group velocity for

a Rossby wave with the wave vector $\boldsymbol{k} = \{k_1, k_2, k_3\}$ in the motionless homogeneously stratified ocean is defined by

$$c_{gz} = \frac{2f_0^2\beta k_1 k_3}{N^2(k_1^2 + k_2^2 + f_0^2 k_3^2/N^2)^2}.$$

An elementary analysis of this formula shows that for a wave with, say, $k_1^{-1} = 1000$ km, $k_3^{-1} = 1000$ m in the mid-latitudes $c_{gz} \approx 1$ km/year (Gill 1982); but this value rapidly decreases with the reduction of the vertical scale, thus making the normal mode approach only marginally applicable.

Another weak point of our approach is the neglect of viscous effects (or, to be more precise, only their implicit inclusion via the prescribed velocity profile). However, this inviscid solution seems to be a useful first step towards the the description of the manifestations mechanism. The problem that completely takes into account viscosity seems to be tractable through direct numerical simulation only and represents the subject of a separate study.

We have so far left out the issue of the absolute amplitudes of the topographically caused disturbances at the surface. This point will be considered in the next section within the framework of a multi-layer model, where the direct solution for an arbitrary step-like profile of $U(z)$ is accessible.

4. The multi-layer model

In order to clarify the role of the set of parameters that characterize the basic flow, we consider the multi-layer model. First we obtain the solution for an arbitrary n-layer model; it is obvious that the properties of the normal mode adjustment to the presence of boundary layers found in the previous section will be accompanied by their counterparts in the multi-layer model. We shall focus our attention on the detailed analysis of the three-layer model with the parameters relevant to those observed in nature.

4.1. *General solution*

The n-layer models are the classical tools of geophysical hydrodynamics (see e.g. Pedlosky 1979). The geometry and notation for the present case are specified in figure 6. We preserve the preceding notation where possible. Each ith layer is characterized by the velocity U_i, pressure p_i and thickness d_i, while the interfaces between layers are described by the vertical displacement η_i and the 'local Burger number'

$$S_i = \frac{gH(\rho_{i+1} - \rho_i)}{f_0^2 L^2 \rho_0}. \tag{4.1}$$

There are n layers and $n-1$ interfaces. We enumerate them from bottom to top, the manner adopted from McCartney (1975). Pressure is non-dimensionalized as follows:

$$p_n = [p_n^* - \rho_n g H(1-z)]/(\rho_0 U_0 f_0 L),$$

$$p_i = \left[p_i^* - gH\sum_{k=i+1}^{n}\rho_k d_k - \rho_i g H\left(\sum_{k=1}^{i} d_k - z\right)\right]/(\rho_0 U_0 f_0 L).$$

Each of the interfaces can be found at

$$z_i^{in} = \sum_{k=1}^{i} d_k + \eta_i. \tag{4.2}$$

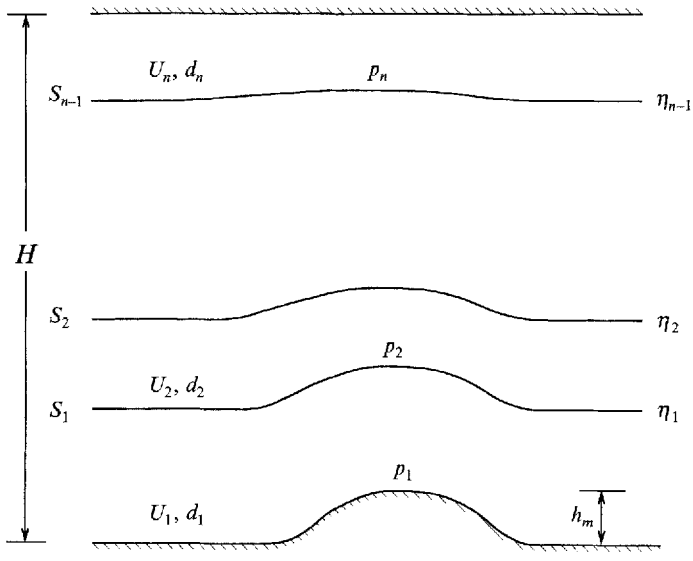

FIGURE 6. Nomenclature for the multi-layer model.

In each layer the quasi-geostrophic vorticity equation

$$\boldsymbol{q}_i \nabla(\nabla_h^2 p_i + \beta y) = (w_i)_z, \quad i = 1, \ldots, n, \tag{4.3}$$

where $\nabla_h^2 = \{\partial^2/\partial x^2, \partial^2/\partial y^2\}$, is fulfilled, and the ideology of the quasi-geostrophic approximation requires the boundary conditions

$$(\boldsymbol{q}_i - \boldsymbol{q}_{i+1})\nabla\eta_i = 0, \quad i = 1, \ldots, n-1 \tag{4.4}$$

to be applied at the undisturbed levels. Doing this, we obtain the system of n equations:

$$\left.\begin{aligned} &\boldsymbol{q}_n \nabla\left[\nabla_h^2 p_n + \beta y + \frac{\eta_{n-1}}{d_n}\right] = 0, \\ &\boldsymbol{q}_i \nabla\left[\nabla_h^2 p_i + \beta y + \frac{\eta_{i-1} - \eta_i}{d_n}\right] = 0, \quad i = 2, \ldots, n-1, \\ &\boldsymbol{q}_1 \nabla\left[\nabla_h^2 p_1 + \beta y + \frac{h}{d_1 \epsilon} - \frac{\eta_1}{d_1}\right] = 0. \end{aligned}\right\} \tag{4.5}$$

As previously, we introduce the disturbance variables ϕ_i, ξ_i, so that $p_i = -U_i y + \phi_i$ and $\eta_i = -(U_i - U_{i+1})y/S_i + \xi_i$, and integrate (4.5) along the streamlines. With

$$\xi_i = (\phi_i - \phi_{i+1})/S_i \tag{4.6}$$

the linear system of the form

$$\left.\begin{aligned} &\nabla_h^2 \phi_1 - P_1 \phi_1 = -\frac{\phi_2}{d_1 S_1} - \frac{h}{d_1 \epsilon}, \\ &\nabla_h^2 \phi_i - P_i \phi_i = -\frac{\phi_{i-1}}{d_i S_{i-1}} - \frac{\phi_{i+1}}{d_i S_i}, \quad i = 2, \ldots, n-1, \\ &\nabla_h^2 \phi_n - P_n \phi_n = -\frac{\phi_{n-1}}{d_n S_{n-1}} \end{aligned}\right\} \tag{4.7}$$

is obtained; this is a counterpart of the continuous problem (3.6), (3.7 *a*, *b*). Here we

denote

$$P_i = -\frac{\beta}{U_i} + \frac{U_{i-1}}{U_i d_i S_{i-1}} + \frac{U_{i+1}}{U_i d_i S_i}, \quad i = 1, \ldots, n,$$

where $U_0 = U_{n+1} = 0$.

The remarks of §2 concerning the possible presence of closed streamlines apply here as well. For consistency with the continuous case we also assume that all U_i are of the same sign, though here the weaker condition may be used; this also guarantees the absence of instability. It is obvious, however, that the fulfillment of requirements underlying the quasi-geostrophic approximation cannot be guaranteed *a priori*.

These requirements are more explicit for the present case and reduce to the condition

$$\xi_i \ll \min(d_i, d_{i+1}); \tag{4.8}$$

this should certainly be verified *a posteriori*.

Since our primary interest lies mainly in the uppermost streamfunction ϕ_n, it is convenient to rewrite the system (4.7) as

$$(\nabla_h^2 + \kappa_1^2)(\nabla_h^2 + \kappa_2^2) \ldots (\nabla_h^2 + \kappa_n^2)\phi_n = \frac{(-1)^n h}{\epsilon d_1 d_2 \ldots d_n S_1 S_2 \ldots S_{n-1}}, \tag{4.9}$$

where κ_i^2 are the eigenvalues of the problem for stationary Rossby waves over a flat bottom. They are found as roots of the algebraic equation

$$a_n \kappa^{2n} + a_{n-1}\kappa^{2n-2} + \ldots + a_0 = 0, \tag{4.10}$$

with the coefficients

$$\left.\begin{aligned} &a_n = 1, \quad a_{n-1} = \sum P_i, \quad a_{n-2} = \sum P_i P_j - \sum Q_i, \quad a_{n-3} = \sum P_i P_j P_k - \sum P_i Q_j, \\ &a_{n-4} = \sum P_i P_j P_k P_l - \sum P_i P_j Q_k + \sum Q_i Q_j, \quad \text{etc.} \end{aligned}\right\} \tag{4.11}$$

Here we have used the notation

$$Q_i = (d_i d_{i+1} S_i^2)^{-1}, \tag{4.12}$$

and it is seen that whilst P_i refers to ith layer, Q_i collects the terms important for the ith interface. This defines the summation instructions for (4.11): the summation is performed for all i, j, k, l from 1 to n, with the requirement that when P_i is multiplied by P_j, i and j should be different; for the terms of the form $P_i Q_j$ the layer should not be adjacent to the interface ($i < j$ or $i > j+1$); for $Q_i Q_j \mid i - j \mid > 1$. It can be shown that all κ_i^2 are real and different.

The solution to (4.9) is straightforward since it is reduced to a combination of the one-layer solutions of Johnson (1977); Long's condition is again required. It is convenient to present the solution, as before, in the form of a convolution

$$\phi_n(x, y) = \int_{-\infty}^{+\infty} \int_{-\infty}^{+\infty} G(x - \xi, y - \eta) h(\xi, \eta)\, \mathrm{d}\xi \mathrm{d}\eta, \tag{4.13}$$

where the Green's function is presented as a sum over the eigenmodes of the multi-layer problem

$$G(x, y) = \frac{(-1)^n}{4\pi^2 \epsilon d_1 d_2 \ldots d_n S_1 S_2 \ldots S_{n-1}} [A_1 G_1 + A_2 G_2 + \ldots + A_n G_n], \tag{4.14}$$

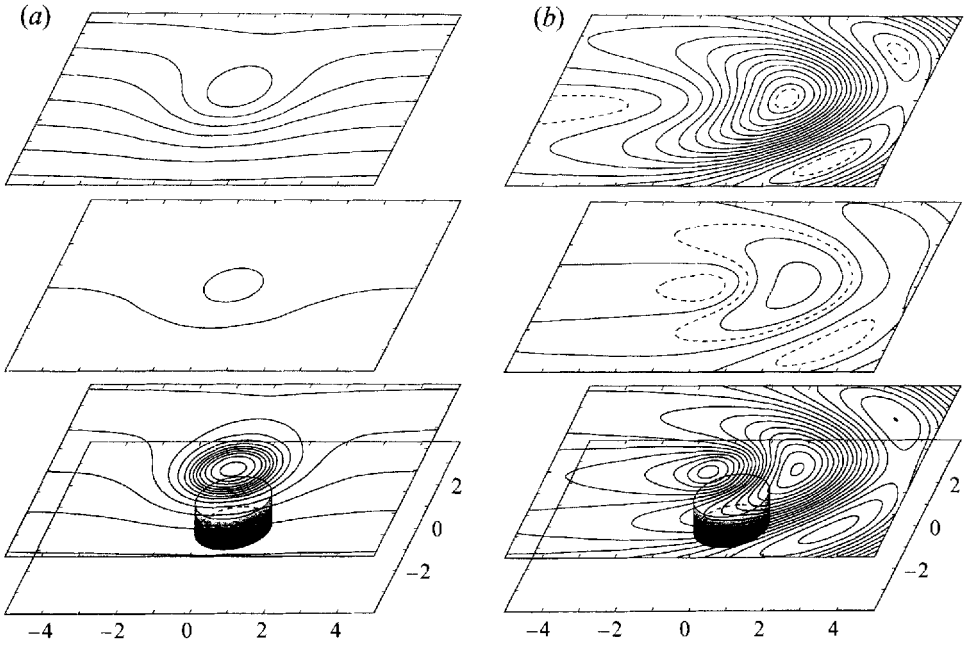

FIGURE 7. Disturbances in the three-layer model with a thick and slow middle layer caused by a cylindrical obstacle. (*a*) Westward current. The parameters values are: $\{U_1, U_2, U_3\} = \{-5, -1, -8\}$ cm s^{-1}, $\{S_1, S_2\} = \{0.6, 5.0\}$, $\{d_1, d_2, d_3\} = \{0.1, 0.87, 0.03\}$, $H = 5000$ m, $h_m = 400$ m, radius of the cylinder is 50 km. Pressure disturbance isolines are shown in steps of 5×10^2 kg m^{-1} s^{-2} (approximately equivalent to 5 cm of water surface elevation). (*b*) Eastward current. As in (*a*) except for the flow direction, $\{U_1, U_2, U_3\} = \{5, 1, 8\}$ cm s^{-1}, and isolines step 10^3 kg m^{-1} s^{-2}.

and each term is defined by

$$G_i(R,\theta) = \begin{cases} -\dfrac{1}{2\pi} K_0(|\kappa_i^2|^{1/2} R), & \kappa_i^2 < 0, \\ \dfrac{1}{4} Y_0(\kappa_i R) + \dfrac{1}{\pi} \displaystyle\sum_{m=0}^{\infty} \frac{\cos[(2m+1)\theta] J_{2m+1}(\kappa_i R)}{2m+1}, & \kappa_i^2 > 0 \end{cases} \tag{4.15}$$

with the coefficients

$$A_i = \left[\prod_{j \neq i} (\kappa_j^2 - \kappa_i^2) \right]^{-1}. \tag{4.16}$$

Again it is understood that $(x, y) = R(\cos\theta, \sin\theta)$, J_m is the Bessel function of the first kind, and Y_0 and K_0 are the Neumann and MacDonald functions, respectively.

4.2. *Three-layer model*

The analysis of the continuous and layered models allowed us to formulate certain general properties of the topographic disturbance and, in particular, to find the mechanism that is responsible for the visibility on the surface of a hydrodynamic image that retains the shape of the topography. Our next aim is to check and go over these results on the basis of a model that could represent the type of vertical structure described above, but at the same time would be characterized by a modest number of parameters. These requirements naturally lead to the choice of a three-layer model, the calculations for this case including only the solution of the cubic equation (4.10)

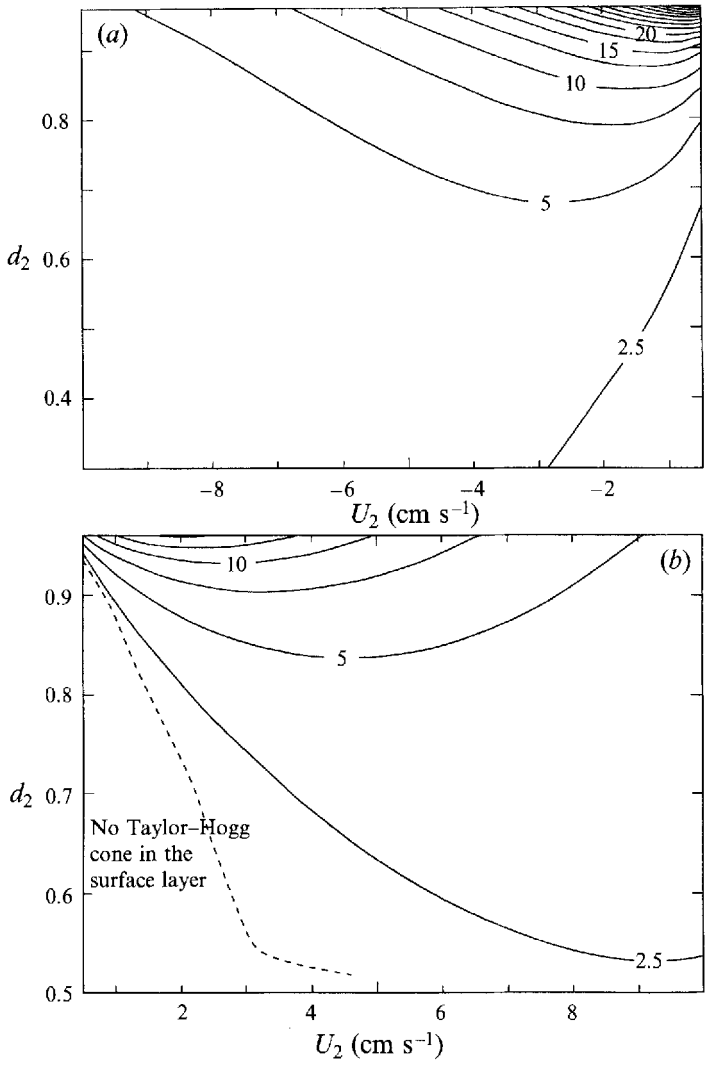

FIGURE 8. Maximum of the pressure disturbance in the uppermost layer (10^2 kg m^{-1} s^{-2}) *vs.* the middle-layer parameters (flow velocity U_2 and thickness d_2): (*a*) westward current, (*b*) eastward current. The other parameters are as in figures 7(*a*) and 7(*b*) respectively.

with $n = 3$. The direct application of the formulae (4.13)–(4.16) for the three modes is elaborated.

The general picture exemplifying the three-layer flow over localized topography is shown in figure 7(*a*, *b*), the cases (*a*) and (*b*) corresponding to westward and eastward flow respectively. For simplicity the topography has been taken to have the form of a cylindrical cap. In both cases the middle layer is thick and almost stagnant, while the thin surface and bottom layers have an order of magnitude larger current. Again, the model is rendered consistent with the continuous case by the requirement that the velocities in all layers have the same sign.

Though the velocities are moderate and confined to the thin layers, it is seen that both the disturbance in the case (*a*) and the part of the disturbance that represents not the wake but the image of the topography in the case (*b*) are pronounced in the surface layer. In the case of the westward current the disturbance is exactly

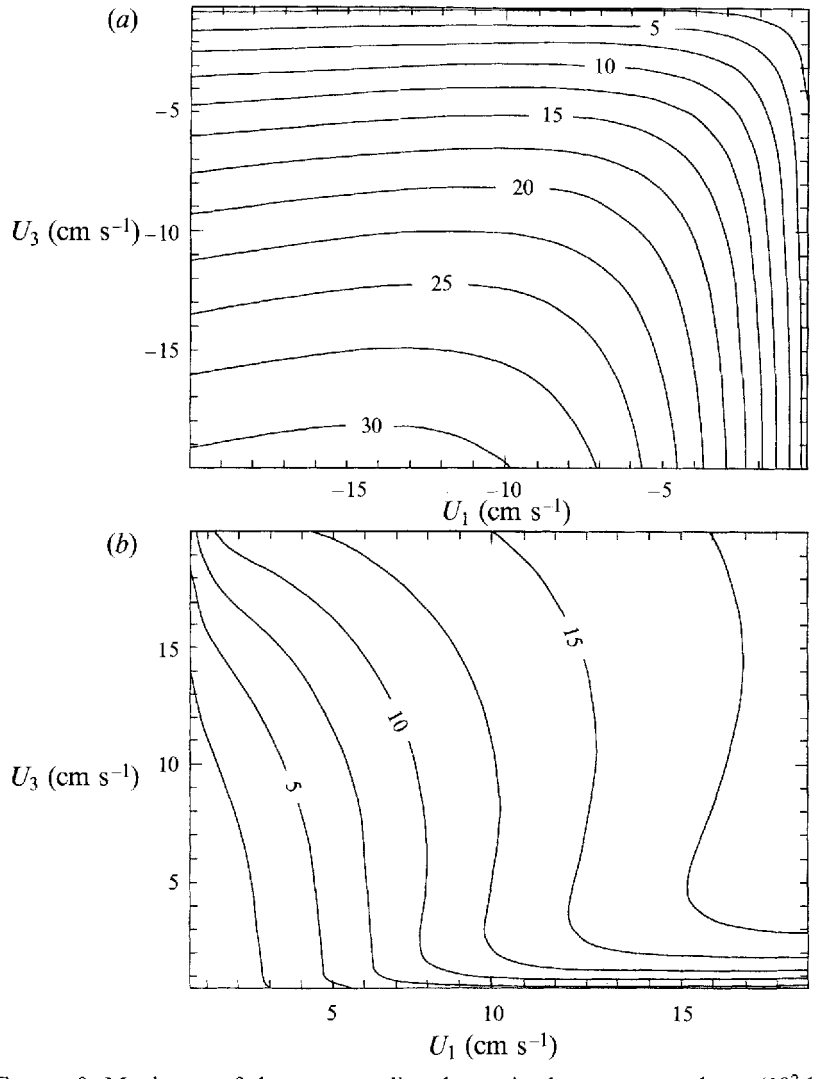

FIGURE 9. Maximum of the pressure disturbance in the uppermost layer (10^2 kg m^{-1} s^{-2}) *vs.* flow velocity in the bottom and surface layers U_1, U_3: (*a*) westward current, (*b*) eastward current. Other parameters are as in figures 7(*a*) and 7(*b*) respectively.

axisymmetric and associated with the region of closed streamlines. However, for the eastward current this image appears to be somewhat weaker and, in addition, is violently distorted by the wake. Since in this particular but characteristic example the only wave-like mode is the barotropic one, the wake is purely barotropic and in fact dominates the surface layer. Nevertheless, the outcrop of the Taylor–Hogg cone, though shifted upstream, is still clearly discernible on the surface.

It is easy to verify that if we replace the current by the equivalent barotropic flow, the stratification will prevent this disturbance from reaching the surface. Moreover, *the surface disturbance diminishes when the small middle layer current is enlarged*. This fact, which appears intuitively to be illogical, is a direct consequence of the theory developed in § 3 and is demonstrated in figure 8 for another particular set of parameters. The disturbance attains its maximum at a certain value of the thick-layer velocity which is much smaller than that of the boundary layers, the phenomenon

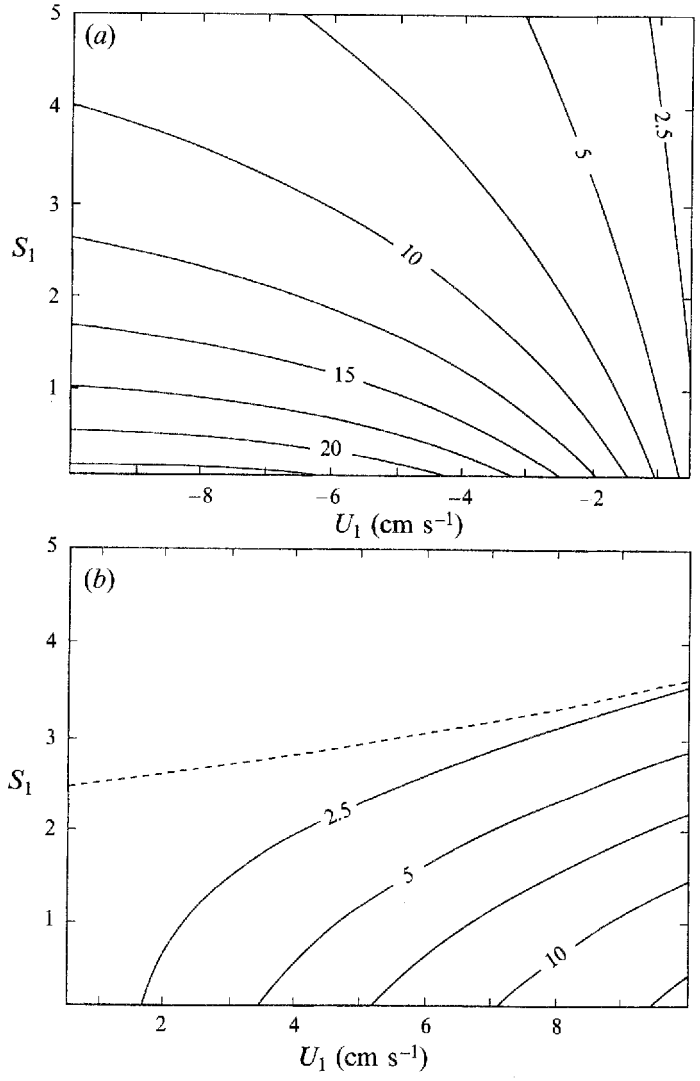

FIGURE 10. Maximum of the pressure disturbance in the uppermost layer (10^2 kg m^{-1} s^{-2}) *vs.* bottom layer current velocity U_1 and the lower interface density jump S_1: (*a*) westward current, (*b*) eastward current. The parameters of figures 7(*a*) and 7(*b*) are again used otherwise.

being clearly attributed to the enhancement mechanism described above. At smaller thick-layer velocities (in this example, less than 1 cm s^{-1}) one of the modes ceases to satisfy the long-wave asymptotic expansion and drastically changes, thus reducing its magnitude at the surface. The situation is more complicated for the eastward current (figure 8*b*), where with the change of the middle velocity the decaying mode can be turned into the wave-like one; the surface pattern then undergoes an abrupt transformation. On the other hand, the disturbance above the topography in the eastward current usually (i.e. for realistic values of parameters) has no closed streamlines, though its magnitude still depends analogously on the middle-layer velocity.

Other parameters important for the enhancement mechanism are the velocity values within the boundary layers, the dependence of the disturbance in each layer on them

being presented in figure 9 (*a, b*). The westward flow disturbance is generally stronger, and its dependence on both velocities is almost identical, being virtually linear for moderate current. For the eastward flow, increasing the surface current above a certain threshold value does not lead to further enhancement, while the dependence in the bottom flow is still practically linear.

Lest the reader get the mistaken impression that the unrealistically high bottom-layer velocity is crucial for the mechanism described, let us consider the dependence of the surface disturbance on the bottom current and the stratification at the lower interface (figure 10). What is really important here is the normal mode increase towards the bottom (see § 3), which is caused, in fact, by the *gradient* of the current velocity, not by its absolute value in the boundary layer.

We conclude this section with a brief remark on the validity of the quasi-geostrophic approximation. In fact, the regimes involved in the present study of the three-layer model require the lower interface to be significantly moved from its undisturbed position, thus formally violating the assumption that this distortion remains small in comparison to the thickness of the lower layer. However, it is important to note that this linear analysis of the multi-layer model is used in this paper for illustrative purposes only, while the continuous model bears less severe limitations due to quasi-geostrophy. On the other hand, we expect that the formal breakdown of the quasi-geostropic approximation within the multi-layer model does not lead to qualitative changes in the disturbance structure, and we hope to confirm this claim in our study of nonlinear ageostrophic regimes which is in progress now.

5. Discussion

Let us summarize the main results of the present paper and briefly discuss their limitations and possible ways of extension.

We have pointed out an effective mechanism responsible for the transmission of large-scale (with the length scales of the order 10^2 km) disturbances from the oceanic bottom to the surface. This mechanism is based upon the existence of shear currents with pronounced near-surface and near-bottom layers. This structure appears to be actually observed in the ocean, though information on the bottom currents and understanding of their dynamics are still fairly incomplete. However, it is important to stress that the value of the current in the lowest 50–100 m of about 2–3 cm s^{-1} seems to be sufficient for the mechanism to work, provided that the bottom layer is separated by a certain density jump. The essence of the mechanism may be expressed in the following way. The eigenmodes of the boundary-value problem, corresponding to the current velocity profile described, have pronounced maxima in the near-bottom and near-surface layers, these maxima leading to effective mode forcing by the topography (the lower maximum) *and* to considerable disturbance in the surface fields (the upper maximum). In quantitative terms the effectiveness means that, say, an underwater hill of a few hundred metres height† in the 4–5 km deep ocean being subjected to an oncoming flow with the mean velocity of 1 cm s^{-1} and a few centimetres per second at the surface and at the bottom, produces:

(i) tilts of the free surface of $O(10^1$ cm per 100 km) which are well within the range of accessibility of modern altimetry;

† Higher underwater mountains are common and one might expect greater manifestations at the surface, but our theory in its present state is utilizing the quasi-geostrophic approximation and therefore we are confined to the consideration of relatively low topography.

(ii) displacements of the thermocline of several dozen metres, which might be *directly visible* provided that there is high plankton concentration in the thermocline and proper lighting conditions (e.g. Pelinovsky 1982);

(iii) perturbations of the surface velocity field of the order of the mean velocity which are, in principle, detectable as well.

Although in this paper we have confined our attention exclusively to the investigation of the hydrodynamic transformation of surface layer, our model could be straightforwardly extended to convert these disturbances into the surface temperature anomalies. This extension seems to be essential for the problem, since the original observations of the bottom topography manifestations dealt with the surface temperature field (see the introduction). Furthermore, present information on the surface temperature in the ocean is fairly complete, thus representing a readily available source of data for the analysis of the manifestation mechanism.

The simplest model of the transformation of near-surface thermocline tilts into disturbances of the surface temperature field can be formulated as follows. Consider an upper mixed layer with an uneven lower boundary, heated (or cooled) from above with the constant heat flux Q. Since the turbulent diffusion coefficient λ is several orders of magnitude larger within a mixed layer than below, it is reasonable to treat the layer as thermally isolated from the rest of the fluid. Neglecting the small horizontal mixing, the heat diffusion within the mixed layer of variable thickness H and initial temperature T_0 can be described by the one-dimensional equation

$$\frac{\partial T}{\partial t} - \lambda \frac{\partial^2 T}{\partial z^2} = 0, \tag{5.1}$$

with the boundary conditions

$$\left.\frac{\partial T}{\partial z}\right|_{z=0} = 0, \qquad \left.\frac{\partial T}{\partial z}\right|_{z=H} = Q \tag{5.2}$$

and the initial condition

$$T(z,0) = T_0. \tag{5.3}$$

Solution to the problem (5.1)–(5.3) can be straightforwardly obtained in the form

$$T = T_0 + \frac{\lambda Q}{H} t + \sum_{n=1}^{\infty} (-1)^n \frac{2QH}{n^2\pi^2} \left[1 - \exp\left(-\lambda \frac{n^2\pi^2}{H^2} t\right)\right] \cos\left(\frac{n\pi}{H} z\right). \tag{5.4}$$

Oceanic observations suggest typical values for the heat flux into the ocean in the range from -10^2 to 10^2 W m^{-2} (Gill 1982); this corresponds to $Q = \pm 2 \times 10^{-3}$ m^{-1}. The diffusion coefficient value for the mixed layer can be taken of the order 10^{-2} m^2 s^{-1} (Pollard 1977), and we shall assume that $H = O(10^2$ m) with variations of the same order. Then on a timescale of 1–2 weeks the exponent in the right-hand side of (5.4) is very close to unity, while the second term gives temperature contrasts of the order $1\text{–}3 \times 10^{-1}$ degrees on the horizontal scale of the variations of H. Note that according to this simple estimate, the value of the temperature disturbance depends on Q and thus may vary and even change sign in different oceanic conditions. The presence of intense high-frequency advective motions may diminish considerably the temperature contrasts found. However, under favourable conditions one may expect the estimate to be adequate.

The problem of establishing the connections between the obtained 'hydrodynamic image' and images in optical and microwave bands seems to be much less straight-

forward, although realizable as well. Even a brief discussion of these problems goes beyond the scope of the present study.

Another point of prime importance that we would like to emphasize is that the surface pattern is related to relief *locally*. Thus one might expect the resemblance of the relief and its surface manifestations in all physical fields despite the fact that the physical mechanisms of transformation of the hydrodynamic image into other characteristics are not established completely yet.

The sensitivity of the results to the basic assumptions is still unclear. The most confining limitation imposed by the quasi-geostrophic approximation we hope to overcome by studying a nonlinear ageostrophic model. (The work is in progress and the results will be reported elsewhere.) The question on the relation between the timescales for the formation of the steady regime that we studied and the formation of the boundary layers of the basic flow requires, strictly speaking, the solving of the self-consistent nonlinear unsteady viscous problem, a task tractable only through extensive direct numerical simulation. However, we hope to get some estimations just from the analysis of the linear unsteady problem.

The presently available data do not allow the direct testing of the theory developed above. We are unaware of any data with the simultaneous measurements of near-surface fields at large scales *and* the currents within the upper and bottom layers. Nevertheless, the existing data demonstrate that the seasonal thermocline displacements due to moderate topography can be of the order of a few dozen metres (see figure 1 *b*), in agreement with the present theory.

We have shown in this paper that the specific vertical structure of the background flow is crucial for the surface signatures of topography. This fact prompts an interesting question: is it possible to reconstruct the vertical flow profile given only the surface observations and topography, provided that the surface manifestations are indeed present and measured with good accuracy? A positive answer would find very important applications in physical oceanography. This *inverse problem* was considered within the frame of the multi-layer model in Annenkov & Shrira (1993) (see also Annenkov & Shrira 1994), where it was found that the inverse problem is well posed for the three-layer model under certain additional assumptions. Thus for the three-layer model a unique solution to the inverse problem was constructed. The possibility of obtaining any information on the deep ocean currents from surface measurements seems to be very alluring and we plan to continue the analysis of this problem. The results will be reported elsewhere.

This work has benefited from the useful discussions with many our colleagues, special thanks being due to L. A. Ostrovsky, G. M. Reznik and V. N. Zyryanov. We are grateful also to referees for their comments. The research was supported by Russian Foundation for Fundamental Research (Grant No. 94-05-17272) and by the International Science Foundation (Grants No. MMP000 and MMP300).

REFERENCES

ANNENKOV, S. YU. & SHRIRA, V. I. 1993 On the reconstruction of flow profiles in the ocean from topographically caused surface anomalies. *Dokl. Russian Akad. Nauk.* **333**, 771–774 (in Russian).

ANNENKOV, S. YU. & SHRIRA, V. I. 1994 Manifestations of bottom topography on the ocean surface: the physical mechanism and solution of direct and inverse problems on a beta-plane. In *Fourth Intl Symp. on Stratified Flows* (ed. E. Hopfinger, B. Voisin & G. Chavand). Preprints, vol. 4. Institut de Méchanique de Grenoble.

BARENBLATT, G. I., GALERKINA, N. L. & LEBEDEV, I. A. 1992 Mathematical model of lower quasi-homogeneous oceanic boundary-layer – general concepts and model of scaling. *Fiz. Atmos. Okeana* **28**, 91–100 (in Russian).

DICKSON, R. R., GOULD, W. S., MÜLLER, T. J. & MAILLARD, C. 1985 Estimates of the main circulation in the deep (> 2000 m) layer of the eastern North Atlantic. *Prog. Oceanogr.* **14**, 103–127.

FUGLISTER, F. C. 1960 *Atlantic Ocean Atlas*. Woods Hole Oceanographic Institution.

GILL, A. E. 1982 *Atmosphere-Ocean Dynamics*. Academic Press.

GNEVYSHEV, V. G. & SHRIRA, V. I. 1990 On the evaluation of barotropic-baroclinic instability parameters of zonal flows on a beta-plane. *J. Fluid Mech.* **221**, 161–181.

GRIMSHAW, R. & YI, Z. 1991 Resonant generation of finite-amplitude waves by the flow of a uniformly stratified fluid over topography. *J. Fluid Mech.* **229**, 603–628.

HOGG, N. G. 1980 Effects of bottom topography on ocean currents. In *Orographic Effects in Planetary Flows* (ed. R. Hide & P. W. White). GARP Publ. Ser. No 23, pp. 167–205. Geneva.

HUPPERT, H. E. & BRYAN, K. 1976 Topographically generated eddies. *Deep-Sea Res.* **23**, 655–679.

ILYIN, M. B. & MELNIKOV, V. A. 1988 On the link between spatial temperature changes and the ocean depth. In *Hydrophysical investigations in the 'Mesopolygon' program* (ed. V. G. Kort), pp. 152–159. Moscow (in Russian).

INGERSOLL, A. P. 1969 Inertial columns and Jupiter's Great Red Spot. *J. Atmos. Sci.* **26**, 744–752.

JANOWITZ, G. S. 1975 The effect of bottom topography on a stratified flow in the beta-plane. *J. Geophys. Res.* **80**, 4163–4168.

JERLOV, N. G. 1968 *Optical Oceanography*. Elsevier.

JOHNSON, E. R. 1977 Stratified Taylor columns on a beta-plane. *Geophys. Astrophys. Fluid Dyn.* **9**, 159–177.

KLEIN, H. 1987 Benthic storms, vortices, and particle dispersion in the deep West European basin. *Deutsche Hydr. Zeitschrift* **40**, 87–139.

MCCARTNEY, M. S. 1975 Inertial Taylor columns on a beta-plane. *J. Fluid Mech.* **68**, 71–96.

MCCARTNEY, M. S. 1976 The interaction of zonal currents with topography with application to the Southern Ocean. *Deep-Sea Res.* **23**, 413–427.

MELNIKOV, V. A. 1988 Low-mode semi-diurnal internal waves near the Middle Atlantic Ridge. In *Oceanological researches* (ed. V. G. Kort & E. M. Morozov), No. 41, pp. 73–82. Moscow (in Russian).

PARAMONOV, A. N. & LEBEDEVA, T. P. 1981 The spatial structure of the oceanic temperature field above the Mid-Atlantic Ridge. In *Surface and Internal Waves*, pp. 20–27. Sevastopol (in Russian).

PEDLOSKY, J. 1979 *Geophysical Fluid Dynamics*. Springer.

PELINOVSKY, E. N. (ed.) 1982 *Large-Scale Internal Waves Effect on the Sea Surface*. Gorky (in Russian).

POLLARD, R. T. 1977 Observations and models of the structure of the upper ocean. In *Modelling and Prediction of the Upper Layers of the Ocean* (ed. E. B. Kraus). Pergamon.

RODEN, G. I. 1991 Mesoscale flow and thermohaline structure around Fieberling seamount. *J. Geophys. Res.* **96**, 16653–16672.

ROONEY, D. M. & JANOWITZ, G. S. 1979 Flow over the Rocky and Andes mountains – application of an analytical model. *J. Atmos. Sci.* **36**, 549–558.

SCHAR, C. & DAVIES, H. C. 1988 Quasi-geostrophic stratified flow over isolated finite-amplitude topography. *Dyn. Atmos. Oceans* **11**, 287–306.

SHRIRA, V. I. 1989 On the subsurface waves in the oceanic upper mixed layer. *Dokl. Akad. Nauk. SSSR* **308**, 732–736 (in Russian; English translation: *Transactions (Doklady) USSR Acad. Sci., Earth Science Sect.* **308**, 276–279).

SHRIRA, V. I. 1993 Surface waves on shear currents: solution of the boundary-value problem. *J. Fluid Mech.* **252**, 565–584.

SOLOMAKHA, V. L. & FEDOROV, K. N. 1983 On possibilities of feature observations of the deep ocean bottom topography from space. *Earth Research from Space*, No. 6, 13–21 (in Russian).

WARREN, B. A. & OWENS, W. B. 1985 Some preliminary results concerning deep northern-boundary currents in the North Pacific. *Prog. Oceanogr.* **14**, 537–551.

ZYRYANOV, V. N. 1985 *The Steady Ocean Currents Theory*. Leningrad (in Russian).